

Published in final edited form as:

Nat Genet. 2014 February ; 46(2): 100–106. doi:10.1038/ng.2876.

## Advantages and pitfalls in the application of mixed model association methods

Jian Yang<sup>1,2,\*</sup>, Noah A. Zaitlen<sup>3,\*</sup>, Michael E. Goddard<sup>4,\*\*</sup>, Peter M. Visscher<sup>1,2,\*\*</sup>, and Alkes L. Price<sup>5,6,7,\*\*</sup>

<sup>1</sup>University of Queensland Diamantina Institute, University of Queensland, Princess Alexandra Hospital, Brisbane, Queensland, Australia

<sup>2</sup>Queensland Brain Institute, University of Queensland, Brisbane, Queensland, Australia

<sup>3</sup>Department of Medicine, Lung Biology Center, University of California San Francisco, San Francisco, California, USA

<sup>4</sup>Faculty of Land and Food Resources, University of Melbourne, Parkville, Victoria, Australia

<sup>5</sup>Department of Epidemiology, Harvard School of Public Health, Boston, Massachusetts, USA

<sup>6</sup>Department of Biostatistics, Harvard School of Public Health, Boston, Massachusetts, USA

<sup>7</sup>Program in Medical and Population Genetics, Broad Institute of MIT and Harvard, Cambridge, Massachusetts, USA

### Abstract

Mixed linear models are emerging as a method of choice for conducting genetic association studies in humans and other organisms. The advantages of mixed linear model association (MLMA) include preventing false-positive associations due to population or relatedness structure, and increasing power by applying a correction that is specific to this structure. An underappreciated point is that MLMA can also increase power in studies without sample structure, by implicitly conditioning on associated loci other than the candidate locus. Numerous variations on the standard MLMA approach have recently been published, with a focus on reducing computational cost. These advances provide researchers applying MLMA methods with many

---

Correspondence should be addressed to P.M.V. (peter.visscher@uq.edu.au) or A.L.P. (aprice@hsph.harvard.edu).

\* Joint first authors.

\*\* Joint senior authors.

#### Author contributions

All authors conceived the project and designed the analyses. J.Y., N.A.Z. and A.L.P. performed the analyses. J.Y., M.E.G. and P.M.V. provided the theoretical derivations. J.Y. wrote the GCTA software. J.Y., N.A.Z. and A.L.P. wrote the manuscript with edits from all authors.

#### Web Resources

GCTA software (GCTA-MLMi and GCTA-LOCO): <http://ctgg.qbi.uq.edu.au/software/gcta/mlmassoc.html>.

EMMAX software: <http://genetics.cs.ucla.edu/emmax/>.

Fast-LMM software: <http://research.microsoft.com/en-us/um/redmond/projects/MSCompBio/Fastlmm/>.

GEMMA software: <http://stephenslab.uchicago.edu/software.html>.

GRAMMAR-Gamma, in GenABEL package of GenABEL project: <http://www.genabel.org> (also see MixABEL package of GenABEL project: same URL).

WTCCC2 data was downloaded from <https://www.wtccc.org.uk/cc2/>.

The NHGRI GWAS catalogue is available at <http://www.genome.gov/gwastudies/>.

options to choose from, but we caution that MLMA methods are still subject to potential pitfalls. Here, we describe and quantify the advantages and pitfalls of MLMA methods as a function of study design, and provide recommendations for the application of these methods in practical settings.

---

## Mixed model association methods prevent false-positive associations and increase power

Mixed linear models are an emerging method of choice when conducting association mapping in the presence of sample structure, including geographic population structure, family relatedness and/or cryptic relatedness<sup>1–12</sup>. The basic approach is to build a genetic relationship matrix (GRM) modeling genome-wide sample structure, estimate its contribution to phenotypic variance using a random-effects model (with or without additional fixed effects), and compute association statistics that account for this component of phenotypic variance (Online Methods). We note that mixed linear models can also be used to estimate components of heritability explained by genotyped markers<sup>13–14</sup>, and to predict complex traits using genetic data<sup>15–16</sup>.

Mixed linear model association (MLMA) methods are effective in preventing false-positive associations due to sample structure in studies of humans and model organisms<sup>1–6</sup>. In particular, simulations show that the correction for confounding is nearly perfect for common variants even when geographic population structure, which is a fixed effect, is modeled as a random effect based on overall covariance<sup>6,17–19</sup> (however, rare variants pose a greater challenge for all methods, due to differential confounding of rare and common variants<sup>20</sup>). MLMA methods also provide an increase in power, by applying a correction that is specific to sample structure<sup>1–6</sup>. In the case of geographic population structure, markers with large allele frequency differences between populations will receive a larger correction. In the case of relatedness structure, the contribution of related individuals to test statistics will be reduced, preventing overweighting of redundant information due to correlation structure.

An underappreciated point is that MLMA can also increase power in studies *without* sample structure, by implicitly conditioning on associated loci other than the candidate locus that are not genome-wide significant in the data being analyzed<sup>8</sup>. For example, a GRM computed from all markers can be used to approximate the set of causal markers (implicitly assuming that all markers are causal), but this approximation can be generalized. The increase in power scales with the ratio  $N/M$  of the number of samples ( $N$ ) to the effective number of independent markers ( $M$ ), since the information about unknown associated loci depends on the number of samples. In simulations of a quantitative trait with no sample structure and no LD between markers (Online Methods), application of MLMA instead of linear regression increased average  $-\log_{10}P$ -values at causal markers from 2.89 to 2.94 (1.8% increase) when  $N=10,000$  and  $M=100,000$ , and from 2.92 to 3.46 (18% increase) when  $N=10,000$  and  $M=10,000$ . We note that this improvement is contingent on the exclusion of the candidate marker from the GRM (see below).

## Reducing the computational cost of mixed model association analysis

In initial implementations of MLMA, the component of phenotypic variance explained by the GRM was estimated separately when testing for the association of each candidate marker. This accounts for the fact that the total variance explained by all markers except the candidate marker may vary across candidate markers, in the case of markers of large effect<sup>1-3</sup>. Even for efficient implementations<sup>3</sup>, this is computationally demanding, with computation time  $O(MN^3)$  where  $M$  is the number of markers and  $N$  is the number of samples, because the variance component estimation is repeated for each candidate marker.

Several computational speedups have subsequently been developed. First, two independent studies observed that if markers have small effects, variance components can be approximated by estimating them only once using all markers (as previously proposed in family-based tests<sup>21</sup>), making MLMA feasible on large datasets<sup>4-5</sup>. Two subsequent studies developed computationally efficient exact methods<sup>7,11</sup>, which do not require variance components to be the same for all candidate markers. Each of these methods enables exact MLMA analysis in computation time  $O(MN^2 + N^3)$ . The difference between approximate and exact methods was reported to be large in a mouse dataset with pervasive relatedness and large effect sizes, but negligible in a human dataset<sup>11</sup>. Another fast approximate method has recently been described<sup>12</sup>. Several of these methods use a single eigendecomposition of the GRM to rotate the data, removing its structure<sup>7,11-12</sup>.

The computation time of each method can be broken down into three steps: (1) building the GRM, (2) estimating variance components, and (3) computing association statistics for each SNP. In Table 1, we list the computational cost of each of these steps for the EMMAX<sup>4</sup>, FaST-LMM<sup>7</sup>, GEMMA<sup>11</sup> and GRAMMAR-Gamma<sup>12</sup> implementations, as well as our GCTA implementation (Online Methods and Web Resources). GRAMMAR-Gamma has the advantage that the cost of step (3) is reduced from  $O(MN^2)$  to  $O(MN)$ , greatly reducing the cost of analyzing a large number of phenotypes. To quantify the computational cost in datasets of realistic size, we benchmarked the running time and memory usage of GCTA using simulations of a quantitative trait without sample structure (Supplementary Note, Supplementary Table 1).

### Pitfall: loss in power when candidate marker is included in GRM

Recent work has shown that inclusion of the candidate marker in the GRM can lead to a loss in power<sup>7-8,22</sup>. This is due to double-fitting the candidate marker in the model, both as a fixed effect tested for association and as a random effect as part of the GRM. Listgarten et al.<sup>8</sup>, who referred to this phenomenon as “proximal contamination”, demonstrated that MLM with candidate marker excluded (MLMe) is the mathematically correct approach, and provided an elegant and efficient algorithm for MLMe analysis (implemented in FaST-LMM software). However, due to computation time or memory constraints (and complexities of LD), MLM with candidate marker included (MLMi) is more commonly applied in practice<sup>22</sup>. It is of interest to quantify the power loss of MLMi vs. MLMe, in order to help guide this choice. In this section, we provide new analytical derivations, validated by simulations, to quantify the reduction in test statistics when MLMi is applied.

### Analytical derivations of mean association statistics ( $\lambda_{\text{mean}}$ )

We assume a set of unrelated samples without population structure or other artifacts. Let  $N$  denote the number of samples,  $M$  denote number of markers, and  $h_g^2$  denote the heritability explained by genotyped and/or imputed markers<sup>13</sup>. We assume markers are unlinked, but the same derivations apply to linked markers if  $M$  denotes the effective number of independent markers, which for humans is approximately 60,000 (ref. <sup>23</sup>; Supplementary Note). We emphasize that it is the effective number of independent markers (not the total number of markers) that matters. Details of each derivation below are provided in the Supplementary Note.

For linear regression (LR), the expected mean of  $\chi^2$  association statistics ( $\lambda_{\text{mean}}$ ) is

$$\lambda_{\text{mean}}(\text{LR})=1+Nh_g^2/M \quad [1]$$

regardless of the genetic architecture of the trait<sup>23</sup>.

For MLMi,  $\lambda_{\text{mean}}$  at markers used to construct the GRM is

$$\lambda_{\text{mean}}(\text{MLMi})=1. \quad [2]$$

This highlights the dangers of using  $\lambda_{\text{mean}}$  (or  $\lambda_{\text{median}}$ ) to assess the presence of population stratification or other artifacts. A researcher who observes lower  $\lambda_{\text{mean}}$  (or  $\lambda_{\text{median}}$ ) for MLMi than for LR might conclude that this is due to correction for confounding, but in fact this result is expected even in the absence of any confounding.

Finally, for MLMe,

$$\lambda_{\text{mean}}(\text{MLMe})=1+\frac{Nh_g^2/M}{1-r^2h_g^2} \quad [3]$$

where  $r^2 \approx Nh_g^2/M$  when  $M > N$ . The ratio of  $\lambda_{\text{mean}}$  between MLMe and MLMi is also

$1+\frac{Nh_g^2/M}{1-r^2h_g^2}$ , which is consistent for causal, null and all markers (Supplementary Table 2). If  $M \gg N$  (i.e.  $r^2$  is small), this is only slightly larger than  $1+Nh_g^2/M$ . The difference between MLMe and MLMi is that MLMe is testing the null hypothesis that the candidate marker has no effect, whereas MLMi is testing the null hypothesis that the candidate marker has an effect size drawn from a normal distribution  $N(0, h_g^2/M)$ .

### Simulations

We compared results of LR, MLMi and MLMe in simulations of a quantitative trait without sample structure, for various values of  $N$  and  $M$  (Online Methods). Our results show that MLMe increased power relative to LR but MLMi reduced power (Table 2, Supplementary Figure 1). The magnitude of these effects was proportional to  $N/M$ , consistent with our

derivations (Table 2, Supplementary Table 3); the power differences are small at  $N=10,000$  and  $M=100,000$ , but it is increasingly common for GWAS to be performed at sample sizes considerably larger than  $N=10,000$ . In all simulations, LR and MLMe had  $\lambda_{\text{mean}}$  at null markers equal to 1.00, but MLMi had  $\lambda_{\text{mean}}$  at *all* markers equal to 1.00 so that MLMi had  $\lambda_{\text{mean}}$  for null markers less than 1.

We also conducted simulations based on real genotypes of 133,036 SNPs on chromosomes 1, 2 and 3 in 10,000 unrelated individuals from data analyzed in ref. <sup>24</sup> (Online Methods). For simplicity, when running MLMe we excluded from the GRM all the SNPs on a chromosome where the candidate SNP was located. Results again show that MLMe increases power relative to LR but MLMi reduces power (Figure 1, Table 2, Supplementary Table 3), consistent with our derivations. The effects are magnified because only a subset of the genome was analyzed, but analogous effects in proportion to  $N/M$  are expected at other values of  $N$  and  $M$ .

In summary, we recommend the use of MLMe in preference to MLMi. An efficient implementation of MLMe via a leave-one-chromosome-out analysis is provided in the GCTA software (GCTA-LOCO; Online Methods). An efficient implementation is also provided in the FaST-LMM software<sup>7-8</sup>.

### **Pitfall: using a small subset of markers in GRM can compromise correction for stratification**

Three recent papers have advocated choosing a subset of markers to include in the GRM when employing MLMA methods<sup>7-8,25</sup>. FaST-LMM<sup>7</sup> uses an equally spaced subset of  $M_R=4,000$  (or 8,000) markers in the GRM, motivated by a computational speedup that reduces computational cost to  $O(M_R^2N)$  when  $M_R < N$ . FaST-LMM-Select<sup>8,25</sup> uses the  $M_T$  markers with most significant linear regression  $P$ -values in the GRM, where  $M_T$  is chosen based on either the first local minimum of the genomic control factor  $\lambda_{\text{median}}$ <sup>8</sup> or the global maximum of out-of-sample prediction accuracy using the resulting GRM<sup>25</sup>. The latter approach allows for the possibility of including all markers in the GRM ( $M_T=M$ ), but is computationally intensive (with a running time >10 times larger than MLMA using all markers) due to the high cost of computing out-of-sample prediction accuracy using all markers; an alternative (described on p.10 of the FaST-LMM version 2.05 user manual) is to choose  $M_T$  based on the first local maximum of out-of-sample prediction accuracy. These approaches have made the valuable observation that a substantial increase in power can be attained by implicitly conditioning only on loci that are relatively likely to be truly associated, motivating a thorough investigation of the impact on correcting for stratification. Below, we evaluate the impact of these choices on both false-positive associations and power. In all of these simulations, we excluded the candidate marker from the GRM (MLMe), consistent with ref. <sup>7-8,25</sup>.

To investigate the number of random markers needed to correct for stratification, we conducted simulations of a quantitative trait with population stratification (Online Methods). Our results indicate that when there is subtle population stratification, a few thousand

random markers are not sufficient to provide a thorough correction for stratification (Figure 2, Supplementary Table 4, Supplementary Note), consistent with previous studies<sup>11,26</sup>.

We also investigated the use of the top  $M_T$  associated markers to correct for stratification. Our results indicate that using the top  $M_T$  associated markers based on the first local minimum of the genomic control factor  $\lambda_{\text{median}}$ <sup>8</sup> may not be effective in correcting for stratification, and can lead to a local minimum in  $\lambda_{\text{median}}$  that is different from the global minimum<sup>25</sup> (Figure 2, Supplementary Note). On the other hand, the ref.<sup>25</sup> approach of using the  $M_T$  top associated markers based on the global maximum of out-of-sample prediction accuracy selected  $M_T=M$  and thus provided an effective correction for stratification in these simulations (but see below).

We now turn to the question of power. We generalized our simulations without sample structure, with fraction  $p=0.05$  or  $p=0.005$  of causal markers, to consider the impact of using the top  $M_T$  associated markers in the GRM, for various values of  $M_T$  (Figure 3). When  $p=0.05$ , there are a large number of causal markers with small effect sizes, so that the top  $M_T$  associated markers do not correspond to the true set of causal markers, and including all markers in the GRM ( $M_T=M$ ) performed best. When  $p=0.005$ , there are a smaller number of causal markers with larger effect sizes, so that the top  $M_T$  associated markers more closely reflect the true set of causal markers, and including only a small subset of top markers in the GRM performed best. Results at other parameter settings show that the optimal strategy depends on both the sample size and the genetic architecture of the trait (Supplementary Table 5, Supplementary Note). The ref.<sup>25</sup> approach of using the  $M_T$  top associated markers based on the global maximum of out-of-sample prediction accuracy selected the value of  $M_T$  that maximized power in each of these simulations, achieving the optimal strategy.

Finally, we explored using the top  $M_T$  associated markers in simulations with both stratification and causal markers. Results on stratification correction were similar to our simulations without causal markers (Supplementary Table 6), and results on power were similar to our simulations with no sample structure (Supplementary Table 7). The ref.<sup>25</sup> approach of using the  $M_T$  top associated markers based on the global maximum of out-of-sample prediction accuracy again selected the value of  $M_T$  that maximized power in these simulations, often at the cost of effective stratification correction. For example, for  $N=10,000$ ,  $M=100,000$ ,  $p=0.005$ , this approach selected  $M_T=300$ , leading to a  $\lambda_{\text{median}}$  of 1.26 (vs. a  $\lambda_{\text{median}}$  of 1.00 if including all markers in the GRM). This highlights the challenge that efforts to maximize power can compromise effective stratification correction.

In summary, based on methods published to date, we recommend that studies of randomly ascertained quantitative traits in which population stratification is a key concern should generally include all markers (except for the candidate marker and markers in LD with the candidate marker) in the GRM. On the hand, the approach of ref.<sup>25</sup> is expected to perform well when maximizing power and correcting for cryptic relatedness are the primary goals, and may also prove useful in the case of differential confounding of rare variants due to spatially localized stratification<sup>27</sup>.

## Pitfall: loss in power in ascertained case-control studies

All methods for mixed model association analysis published to date assume that study samples are randomly ascertained with respect to the phenotype of interest. While this is usually true for quantitative phenotypes, it is not true for case-control studies, which generally oversample disease cases to increase study power. Recent work has highlighted the loss in power that occurs in ascertained case-control studies when genetic or clinical covariates are modeled as fixed effects without accounting for ascertainment, and a subset of these studies have developed new methods to address this problem<sup>28–32</sup>. However, the issue of power loss due to ascertainment has not previously been investigated for MLMA, which models both known and unknown associated markers as random effects.

We conducted simulations to investigate the use of existing MLMA methods in ascertained case-control studies. We extended our simulations without sample structure to simulate different values of disease prevalence  $f$  via the liability threshold model<sup>33</sup> (Online Methods). Results for MLMe vs. linear regression show that, for large  $N/M$  and small  $f$ , MLMe can suffer a substantial loss in power (Table 3). Similar results were obtained for different values of  $p$  (the fraction of non-candidate markers that are causal) and the proportion of variance explained by each candidate marker (Supplementary Table 8). We further note that, for large  $N/M$  and small  $f$ , the heritability explained by genotyped markers ( $h_g^2$ ) is mis-estimated by MLMe, even after accounting for observed vs. liability scale with correction for case-control ascertainment<sup>34</sup>. However, using the correct value of  $h_g^2$  does not ameliorate the loss in power (Supplementary Note and Supplementary Table 9).

In summary, MLMA can suffer a severe loss in power due to case-control ascertainment, motivating further research on MLMA methods in case-control samples. The choice of whether to apply MLMA or other methods should be a function of sample size and severity of case-control ascertainment.

## Advantages and pitfalls of MLMA in two empirical case-control studies

We investigated the advantages and pitfalls of MLMA in two recent GWAS of multiple sclerosis (MS) and ulcerative colitis (UC) involving over 20,000 samples<sup>22,35</sup>. We chose these studies for several reasons. First, the MS study was the first large GWAS conducted using MLMA methods. Second, the authors of that study recognized that inclusion of candidate markers in the GRM (MLMi) was a potential pitfall, although analyses were conducted using MLMi based on available methods and software. Third, due to the large sample sizes, these were ideal datasets for exploring the issues highlighted by our simulations.

We analyzed data from 10,204 MS cases and 5,429 controls genotyped on Illumina arrays<sup>22</sup> (Online Methods). This subset of cases and controls were not matched for ancestry (in contrast to ref. <sup>22</sup>), and exhibit substantial population stratification. We retained unmatched samples to maximize the sample size, which we believe is appropriate for these analyses. We also analyzed data from 2,697 UC cases and 5,652 controls genotyped on Affymetrix arrays<sup>35</sup> (Online Methods).

We compared seven methods of computing association statistics: linear regression (LR), LR with 5 PC covariates<sup>26</sup> (PCA), MLMi, MLMe, FaST-LMM using  $M_R=4,000$  random markers<sup>7</sup> (FaST-4K), FaST-LMM-Select using top  $M_T$  markers based on first local minimum of  $\lambda_{\text{median}}$ <sup>8</sup> (FaST-Top), and FaST-LMM-Select using top  $M_T$  markers based on the first local maximum of out-of-sample prediction accuracy using the resulting GRM (FaST-TopX). For each method, we computed average  $\chi^2$  association statistics at all markers and at 75 and 24 known associated markers for MS and UC respectively (Online Methods).

We first consider genome-wide average  $\chi^2$  values (Table 4 and Supplementary Table 10). For MS, the genome-wide value of 0.994 for MLMi is consistent with our derivations and simulations (Table 2), as is the value of 1.232 for MLMe if the effective number of markers is  $M=60,000$  and the heritability explained by genotyped markers is  $h_g^2=0.266$  on the liability scale (0.757 on the observed scale<sup>34</sup>, assuming disease prevalence 0.1%), which is a plausible value given the liability-scale  $h_g^2=0.30 \pm 0.03$  estimated in ref. <sup>36</sup> using independent data. For UC, we observed a genome-wide value of 0.998 for MLMi and 1.100 for MLMe, consistent with  $h_g^2=0.244$  on the liability scale (0.695 on the observed scale) given the lower sample size. The average  $\chi^2$  for PCA was similar to that of MLMe for both traits. Thus, for both MLMe and PCA, the observed inflation in test statistics is consistent with polygenic effects according to our derivations, simulations, and independently obtained estimates of  $h_g^2$ . A higher value for PCA than for MLMi does not necessarily imply that PCA fails to correct for population structure (as suggested by ref. <sup>22</sup>), because our derivations and simulations show that correctly calibrated test statistics are expected to have a higher average  $\chi^2$  than MLMi under a polygenic model. On the other hand, FaST-4K, FaST-Top and FaST-TopX generally exhibit average  $\chi^2$  values that are higher than PCA and MLMe, consistent with an incomplete correction for stratification (Figure 2, Supplementary Tables 4 and 6). Although it is theoretically possible that the higher average  $\chi^2$  for these methods could be entirely due to higher average  $\chi^2$  at causal markers, this is unlikely given that the methods attain relatively similar average  $\chi^2$  at known associated markers (see below).

We also tried running FaST-LMM-Select using top  $M_T$  markers based on the global maximum of out-of-sample prediction accuracy<sup>25</sup>. Our runs failed to complete, because the 96GB memory limit was exceeded. The authors of ref. <sup>25</sup> have reported that running this approach to completion on the same data results in every marker being selected for both MS and UC, and obtains results identical to MLMe (D. Heckerman and O. Weissbrod, personal communication).

We next consider  $\chi^2$  values at known associated markers (Table 4 and Supplementary Table 11). Among methods attaining a complete correction for stratification, MLMe consistently produced higher  $\chi^2$  values than MLMi for both MS (70 of 75 markers;  $P=1 \times 10^{-15}$ ) and UC (24 of 24 markers;  $P=1 \times 10^{-7}$ ), consistent with simulations (Figure 1). MLMe also produced higher  $\chi^2$  values than FaST-Top for UC (18 of 24 markers;  $P=0.02$ ), the only instance in which FaST-4K, FaST-Top or FaST-TopX attained a complete correction for stratification. However, the comparison between MLMe and PCA was inconclusive, with MLMe producing higher values for MS (43 of 75 markers;  $P=0.25$ ) and PCA producing higher



values for UC (13 of 24 markers;  $P=0.84$ ). Due to the lower correlation between these methods, these comparisons are noisy, and analyses of additional datasets will be needed to conclusively distinguish the performance of MLMe vs. PCA in empirical data. We note that the much lower  $\chi^2$  values for MLMi vs. PCA at known associated markers are consistent with ref. <sup>22</sup>, who attributed this to structure that is not captured by PCA. However, the pitfalls of MLMi (Figure 1) provide an alternative explanation.

## Recommendations and future directions

MLMA methods can prevent false-positive associations and increase power, at reasonable computational cost. However, our theoretical derivations, simulations and application to empirical data show that potential pitfalls include including the candidate marker in the GRM, using a small subset of markers in the GRM, and effects of case-control ascertainment.

We recommend excluding candidate markers from the GRM (MLMe) in preference to including them (MLMi). This can be efficiently implemented via a leave-one-chromosome-out analysis<sup>7</sup>, implemented in the GCTA software (GCTA-LOCO; Online Methods). An efficient implementation is also provided in the FaST-LMM software<sup>7-8</sup>. Our analytical derivations demonstrate the advantages of MLMe over MLMi, and also quantify the expected inflation in MLMe test statistics in the absence of confounding, potentially ameliorating the need to apply an additional round of Genomic Control<sup>37</sup> correction as in many recent studies<sup>38</sup>. However, distinguishing between polygenic effects and incomplete correction for stratification is an important direction of future research (B. Bulik-Sullivan, N. Patterson, A.L.P., M. Daly, B. Neale, unpublished data).

We recommend that studies of randomly ascertained quantitative traits should generally include all markers (except for the candidate marker and markers in LD with the candidate marker) in the GRM, except as follows. First, the set of markers included in the GRM can be LD-pruned to reduce running time (with association statistics still computed for all markers). Second, genome-wide significant markers of large effect should be conditioned out as fixed effects<sup>4,9</sup>. Third, when population stratification is less of a concern, we recommend the ref. <sup>25</sup> approach of using the  $M_T$  top associated markers based on the global maximum of out-of-sample prediction accuracy. (This approach may choose either a subset of markers ( $M_T < M$ ) or all markers ( $M_T = M$ ), but computational constraints may preclude the latter choice.) Finally, a potentially appealing way to capture the power advantages of selecting a subset of SNPs to include in the GRM while addressing concerns about stratification is to employ FaST-LMM-Select + PCs (G. Tucker, A.L.P., B. Berger, unpublished data and D. Heckerman, C. Lippert, J. Listgarten and O. Weissbrod, personal communication).

Ascertained case-control studies present a special challenge due to the potential loss in power of standard MLMA methods. When sample size is small or disease prevalence is high, standard MLMA methods can be used (Table 3). Otherwise, in datasets with no relatedness structure, PCA can be used<sup>26</sup>. (In this case, conditioning on genome-wide significant markers or other covariates of large effect can be either omitted<sup>31</sup>, or retained using methods that explicitly model case-control ascertainment to increase power<sup>28-30,32</sup>.)

In ascertained case-control datasets with relatedness structure, we know of no good alternative to MLMA.

We conclude by highlighting three areas in mixed model association analysis in which there is a pressing need for development of new methods. First, there is a need for MLMA methods for ascertained control-traits that do not suffer a loss in power. Second, there is a need for MLMA methods that use mixture distributions of prior effect sizes to increase their power, mirroring advances in phenotypic prediction of livestock and human traits using Bayesian methods<sup>39-41</sup>. Third, further work is needed to develop and assess methods for rare variants, which pose a greater challenge for all methods<sup>20,27</sup>.

## Online Methods

### GCTA implementation of MLMi (GCTA-MLMi)

The phenotype  $\mathbf{y}$  is modeled as

$$\mathbf{y} = \mathbf{K}\mathbf{c} + \mathbf{g} + \mathbf{e} \quad [\text{Model 1}]$$

where  $\mathbf{c}$  is a vector of fixed covariates (including the affine term) with corresponding coefficient matrix  $\mathbf{K}$ ;  $\mathbf{g}$  is a vector of genetic effects with  $\mathbf{g} \sim N(0, \mathbf{A}\sigma_g^2)$ ;  $\mathbf{A}$  is the GRM

defined by  $A_{jk} = \frac{1}{M} \sum_{i=1}^M \frac{(x_{ij} - 2p_i)(x_{ik} - 2p_i)}{2p_i(1-p_i)}$ , where  $x_{ij} = 0, 1$  or  $2$  and  $M$  is the total number of autosomal markers; and  $\mathbf{e}$  is a vector of non-genetic effects with  $\mathbf{e} \sim N(0, \mathbf{I}\sigma_e^2)$ . We note that this is the same GRM used in previous work on principal components analysis<sup>26</sup>. The variance explained by the GRM ( $\sigma_g^2$ ), the noise variance ( $\sigma_e^2$ ) and the heritability explained by genotyped markers ( $h_g^2 = \sigma_g^2 / (\sigma_g^2 + \sigma_e^2)$ ) can be estimated via restricted maximum likelihood (REML)<sup>13,42</sup>. Association statistics are computed by comparing the causal model with an effect at the candidate marker to the null model with no effect at the candidate marker, for example via a generalized least squares (GLS)  $F$ -test or  $\chi^2$  score test<sup>4</sup>.

We then test the effect of SNP  $i$  based on the model

$$\mathbf{y} = \mathbf{K}\mathbf{c} + \mathbf{w}_i b_i + \mathbf{g} + \mathbf{e} \quad [\text{Model 2}]$$

where  $\mathbf{w}_i$  is a vector of mean-adjusted genotypes, i.e.  $w_{ij} = x_{ij} - 2p_i$ . The fixed effects, including both the effects of the covariates and the effect of SNP  $i$ , are estimated by GLS, i.e.  $\hat{\mathbf{q}} = (\mathbf{Q}^T \mathbf{V}^{-1} \mathbf{Q})^{-1} \mathbf{Q}^T \mathbf{V}^{-1} \mathbf{y}$  with  $\text{var}(\hat{\mathbf{q}}) = (\mathbf{Q}^T \mathbf{V}^{-1} \mathbf{Q})^{-1}$ , where  $\mathbf{q} = [\mathbf{c}^T : b_i]^T$ ,  $\mathbf{Q} = [\mathbf{K} : \mathbf{w}_i]$  and  $\mathbf{V} = \mathbf{A}\sigma_g^2 + \mathbf{I}\sigma_e^2$ . The test-statistic is calculated as  $\chi^2 = \hat{b}_i^2 / \text{var}(\hat{b}_i)$ , where  $\text{var}(\hat{b}_i)$  the last diagonal entry of  $(\mathbf{Q}^T \mathbf{V}^{-1} \mathbf{Q})^{-1}$ . Assuming that the proportion of variance explained by a single SNP is small, the estimates of  $\sigma_g^2$  and  $\sigma_e^2$  from [Model 1] will be very similar to those from [Model 2]. To decrease the computational burden, we estimate  $\sigma_g^2$  and  $\sigma_e^2$  once based on [Model 1], without any SNPs included in the fixed effect vector  $\mathbf{c}$ , and use them for effect size estimation and significance testing of each SNP based on [Model 2]; this is an approximate approach similar to that implemented in EMMA<sup>4</sup>. If there are no covariates,

the vector  $\mathbf{c}$  will become a scalar (i.e. the affine term). In this case, for ease of computation, we can adjust the phenotype as  $\mathbf{y}^* = \mathbf{y} - \mathbf{1}\hat{c}$  with  $\hat{c} = (\mathbf{1}^T \mathbf{V}^{-1} \mathbf{1})^{-1} \mathbf{1}^T \mathbf{y}$  and simplify the estimation of SNP effect as  $\hat{b}_i = \mathbf{w}_i^T \mathbf{V}^{-1} \mathbf{y}^* / (\mathbf{w}_i^T \mathbf{V}^{-1} \mathbf{w}_i)$  with  $\text{var}(\hat{b}_i) = 1 / (\mathbf{w}_i^T \mathbf{V}^{-1} \mathbf{w}_i)$ . However, when there are covariates fitted in the models, we estimate the effects of the covariates and the SNP jointly rather than using the simplified approach. This is because if the covariates and the SNP genotype are correlated and the phenotype is pre-adjusted by the covariates, the power of detecting the SNP effect can be reduced. To improve computational efficiency, the efficient computational libraries EIGEN, BLAS and LAPACK are used for linear algebra calculation, and the parallel computing technique OpenMP is used for multi-thread computing.

### GCTA implementation of MLMe via LOCO analysis (GCTA-LOCO)

This implementation is identical to GCTA-MLMi, except that markers on a given autosome are evaluated using a GRM constructed from the remaining autosomes, via pre-computing and storing the GRM constructed from all autosomes. GCTA-LOCO attains running time and memory usage only 2–3× higher than GCTA-MLMi (Supplementary Table 1).

### Simulations of a quantitative trait with no sample structure

We simulated phenotypes for  $N$  samples using  $M$  non-candidate markers plus 500 candidate markers. All simulations used  $N=10,000$  and  $M=100,000$  unless otherwise specified. (We also included simulations at smaller values of  $N$  and  $M$ , in order to understand how the relative performance of different methods varies with  $N$  and  $M$ .) Allele frequencies were uniformly distributed on  $[0.1, 0.9]$ . The  $M$  non-candidate markers included  $Mp$  causal markers ( $p=0.05$  unless otherwise specified) explaining 50% of the variance of the trait, with normalized effect sizes  $\sim N(0, 0.5/Mp)$ . The 500 candidate markers explained an additional 50% of the variance of the trait, with normalized effect sizes  $\sim N(0, 0.5/500)$ . We ran MLMe by including the  $M$  non-candidate markers in the GRM and testing only the 500 candidate markers. We ran MLMi by including the  $M$  non-candidate markers plus the 500 candidate markers in the GRM. Thus, the heritability explained by markers included in the GRM was 50% for MLMe and 100% for MLMi.

### Yang et al. 2011 data and simulated phenotypes

We analyzed data from 14,347 individuals from the ARIC, HPFS and NHS cohorts that were genotyped using Affymetrix 6.0 arrays at 565,040 autosomal markers after quality control, as described previously<sup>24</sup>. Informed consent was obtained from all subjects. We excluded one of each pair of individuals with genetic relatedness  $>0.025$  in the GRM, leaving 11,586 unrelated individuals. We selected a random subset of 10,000 unrelated individuals. We restricted to 45,772 markers on chr1, 47,596 markers on chr2 and 39,668 markers on chr3, for a total of  $M=133,036$  markers. We randomly selected 200 causal markers (100 each on chr1 and chr2) explaining 50% of the variance of the trait, with normalized effect sizes  $\sim N(0, 0.5/200)$ . We ran MLMi by including all markers in the GRM (GCTA-MLMi), and ran MLMe using a GRM estimated from the remaining chromosomes (GCTA-LOCO). We included causal markers on two different chromosomes in order to assess the benefit of running MLMe using a GRM containing causal markers on a different

chromosome, and included a third chromosome with no causal markers in order to assess association statistics at markers that are not causal and not in LD with a causal marker.

### Simulations of a quantitative trait with population stratification

We simulated phenotypes for  $N/2$  samples from each of two discrete subpopulations, based on a mean trait difference of 0.25 standard deviations between subpopulations with no causal marker effects. We simulated  $M$  markers for the GRM plus 500 additional candidate markers, based on  $F_{ST}=0.005$  or  $F_{ST}=0.0025$  between subpopulations. Ancestral allele frequencies  $x$  were uniformly distributed on  $[0.1,0.9]$ , and subpopulation allele frequencies were sampled from a beta distribution with parameters  $x(1-F_{ST})/F_{ST}$  and  $(1-x)(1-F_{ST})/F_{ST}$ , which has mean  $x$  and variance  $F_{ST}x(1-x)$ . Causal markers in simulations with both stratification and causal markers were simulated in the same way as in simulations with no sample structure (see above).

### Simulations of ascertained case-control traits

We simulated normally distributed liabilities, transformed liabilities to case-control status by defining individuals with liability  $>T$  to be cases and others to be controls (where the liability threshold  $T$  is chosen to achieve a specified disease prevalence  $f$ ), and continued in this fashion until  $N/2$  cases and  $N/2$  controls were generated. Liabilities were simulated as in the simulations of a quantitative trait with no sample structure, except that liability-scale effect sizes of the 5 candidate markers were chosen so that each candidate marker explains the proportion  $10/N$  of observed-scale variance, after accounting for the transformation between variance explained on the liability scale vs. the observed scale with correction for case-control ascertainment<sup>34</sup>. We used only 5 candidate markers so as to limit the liability-scale variance explained by the candidate markers, which exceeds observed-scale variance when prevalence is low. We also included  $M$  non-candidate markers, of which the proportion  $p$  were causal ( $p=0.05$  or  $p=0.005$ ) and explained 50% of the liability-scale variance. To examine results for candidate markers of larger effect, we repeated all simulations with each candidate marker explaining the proportion  $20/N$  of observed-scale variance.

### MS and UC datasets

We analyzed data from 10,204 MS cases and 5,429 controls (from NBS and 1958BC) genotyped on Illumina arrays made available to researchers via WTCCC2 (see Web Resources). Although ref. <sup>22</sup> analyzed UK and non-UK samples separately followed by meta-analysis in most of their analyses, the data made available to researchers includes both UK and non-UK cases but only UK controls. We retained all samples in order to maximize sample size. We considered markers that were present in each of MS, NBS and 1958 BC datasets and removed markers with  $>0.5\%$  missing data,  $P<0.01$  for allele frequency difference between NBS and 1958BC,  $P<0.05$  for deviation from Hardy-Weinberg equilibrium,  $P<0.05$  for differential missingness between cases and controls, or  $MAF<0.1\%$  in any dataset, leaving 360,557 markers. We employed filters more stringent than in a standard GWAS so as to minimize the impact of assay artifacts on our results<sup>34</sup>. The 75 known associated markers were defined by including, for each MS-associated marker listed

in the NHGRI GWAS catalogue (see Web Resources), a single best tag at  $r^2 > 0.4$  from the set of 360,557 markers if available.

We also analyzed data from 2,697 UC cases and 5,652 controls (from NBS and 1958BC) genotyped on Affymetrix arrays<sup>35</sup> and made available to researchers via WTCCC2. The MS and UC datasets contain overlapping control samples. We employed stringent QC filters as described above, leaving 458,560 markers. The 24 known associated markers were defined by, for each UC-associated marker listed in the NHGRI GWAS catalogue, a single best tag at  $r^2 > 0.4$  from the set of 458,560 if available.

PCA refers to PC correction using 5 PCs. Correction using 10 PCs (PCA10) or 20 PCs (PCA20) was also evaluated (Supplementary Table 10). FaST-4K was run by including  $M_R=4,000$  random markers in the GRM. FaST-Top was run by including the top  $M_T$  markers based on first local minimum of  $\lambda_{\text{median}}$ <sup>8</sup>, using a grid search from 100 to 3,000 with a step size of 100. FaST-TopX was run using the command “fastlmmc -autoSelect <outfile> -randomSeed 1 -autoSelectFolds 10 -bfilesim <indata> -pheno <inpheno> -mphenos 1 -autoSelectSearchValues ASvalues.txt -topKbyLinReg 10000 -memoryFraction 0.2”, as described on p.10 of the FaST-LMM version 2.05 user manual. (The -topKbyLinReg 10000 option was not used in our simulations, which selected the global optimum of  $M_T$ .) FaST-Top selected  $M_T=2,000$  top markers for MS and  $M_T=400$  top markers for UC, and FaST-TopX selected  $M_T=2,800$  top markers for MS and  $M_T=3$  top markers for UC.

## Supplementary Material

Refer to Web version on PubMed Central for supplementary material.

## Acknowledgments

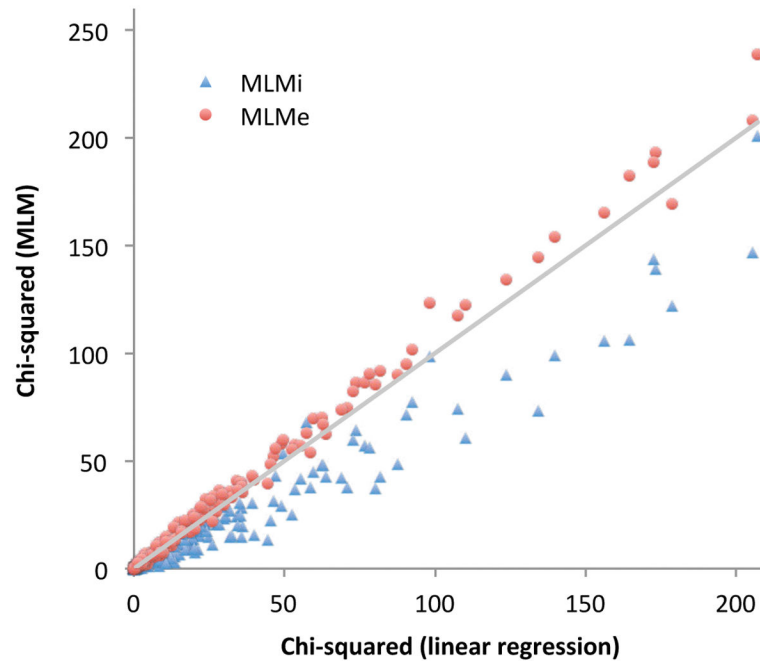
We are grateful to N. Patterson, D. Heckerman, J. Listgarten, C. Lippert, E. Eskin, B. Vilhjalmsson, P. Loh, T. Hayeck, T. Frayling, A. McRae, L. Ronnegard, O. Weissbrod, G. Tucker and the GIANT consortium for helpful discussions and to A. Gusev and S. Pollack for assistance with the MS and UC datasets. We are grateful to two anonymous referees for their helpful comments. This study makes use of data generated by the Wellcome Trust Case-Control Consortium and data from Yang et al. 2011 obtained from dbGaP through accession numbers [phs000090] and [phs000091] (see Supplementary Note for the full set of acknowledgements for this data). This research was supported by NIH grants R01 HG006399, GM099568 and GM075091, by the Australian Research Council (DP130102666) and by the Australian National Health and Medical Research Council (APP1011506 and APP1052684).

## References

1. Yu J, et al. A unified mixed-model method for association mapping that accounts for multiple levels of relatedness. *Nat Genet.* 2006; 38:203–8. [PubMed: 16380716]
2. Zhao K, et al. An Arabidopsis example of association mapping in structured samples. *PLoS Genet.* 2007; 3:e4. [PubMed: 17238287]
3. Kang HM, et al. Efficient control of population structure in model organism association mapping. *Genetics.* 2008; 178:1709–23. [PubMed: 18385116]
4. Kang HM, et al. Variance component model to account for sample structure in genome-wide association studies. *Nat Genet.* 2010; 42:348–54. [PubMed: 20208533]
5. Zhang Z, et al. Mixed linear model approach adapted for genome-wide association studies. *Nat Genet.* 2010; 42:355–60. [PubMed: 20208535]

6. Price AL, Zaitlen NA, Reich D, Patterson N. New approaches to population stratification in genome-wide association studies. *Nat Rev Genet.* 2010; 11:459–463. [PubMed: 20548291]
7. Lippert C, et al. FaST linear mixed models for genome-wide association studies. *Nat Methods.* 2011; 8:833–5. [PubMed: 21892150]
8. Listgarten J, et al. Improved linear mixed models for genome-wide association studies. *Nat Methods.* 2012; 9:525–6. [PubMed: 22669648]
9. Segura V, et al. An efficient multi-locus mixed-model approach for genome-wide association studies in structured populations. *Nat Genet.* 2012; 44:825–830. [PubMed: 22706313]
10. Korte A, et al. A mixed-model approach for genome-wide association studies of correlated traits in structured populations. *Nat Genet.* 2012; 44:1066–71. [PubMed: 22902788]
11. Zhou X, Stephens M. Genome-wide efficient mixed-model analysis for association studies. *Nat Genet.* 2012; 44:821–4. [PubMed: 22706312]
12. Svishcheva GR, Axenovich TI, Belonogova NM, van Duijn CM, Aulchenko YS. Rapid variance components-based method for whole-genome association analysis. *Nat Genet.* 2012; 44:1166–70. [PubMed: 22983301]
13. Yang J, et al. Common SNPs explain a large proportion of the heritability for human height. *Nat Genet.* 2010; 42:565–9. [PubMed: 20562875]
14. Zaitlen N, Kraft P. Heritability in the genome-wide association era. *Hum Genet.* 2012; 131:1655–64. [PubMed: 22821350]
15. Henderson CR. Best linear unbiased estimation and prediction under a selection model. *Biometrics.* 1975; 31:423–47. [PubMed: 1174616]
16. de los Campos G, Gianola D, Allison DB. Predicting genetic predisposition in humans: the promise of whole-genome markers. *Nat Rev Genet.* 2010; 11:880–6. [PubMed: 21045869]
17. Sul JH, Eskin E. Mixed models can correct for population structure for genomic regions under selection. *Nat Rev Genet.* 2013; 14:300. [PubMed: 23438871]
18. Price AL, Zaitlen NA, Reich D, Patterson N. Response to Sul and Eskin. *Nat Rev Genet.* 2013; 14:300. [PubMed: 23438870]
19. Wang K, Hu X, Peng Y. An Analytical Comparison of the Principal Component Method and the Mixed Effects Model for Association Studies in the Presence of Cryptic Relatedness and Population Stratification. *Hum Hered.* 2013; 76:1–9. [PubMed: 23921716]
20. Mathieson I, McVean G. Differential confounding of rare and common variants in spatially structured populations. *Nat Genet.* 2012; 44:243–6. [PubMed: 22306651]
21. Chen WM, Abecasis GR. Family-based association tests for genomewide association scans. *Am J Hum Genet.* 2007; 81:913–26. [PubMed: 17924335]
22. Sawcer S, et al. Genetic risk and a primary role for cell-mediated immune mechanisms in multiple sclerosis. *Nature.* 2011; 476:214–9. [PubMed: 21833088]
23. Yang J, et al. Genomic inflation factors under polygenic inheritance. *Eur J Hum Genet.* 2011; 19:807–12. [PubMed: 21407268]
24. Yang J, et al. Genome partitioning of genetic variation for complex traits using common SNPs. *Nat Genet.* 2011; 43:519–25. [PubMed: 21552263]
25. Lippert C, et al. The benefits of selecting phenotype-specific variants for applications of mixed models in genomics. *Sci Rep.* 2013; 3:1815. [PubMed: 23657357]
26. Price AL, et al. Principal components analysis corrects for stratification in genome-wide association studies. *Nat Genet.* 2006; 38:904–9. [PubMed: 16862161]
27. Listgarten J, Lippert C, Heckerman D. FaST-LMM-Select for addressing confounding from spatial structure and rare variants. *Nat Genet.* 2013; 45:470–1. [PubMed: 23619783]
28. Mefford J, Witte JS. The Covariate’s Dilemma. *PLoS Genet.* 2012; 8:e1003096. [PubMed: 23162385]
29. Zaitlen N, et al. Analysis of case-control association studies with known risk variants. *Bioinformatics.* 2012; 28:1729–1737. [PubMed: 22556366]
30. Clayton D. Link functions in multi-locus genetic models: implications for testing, prediction, and interpretation. *Genet Epidemiol.* 2012; 36:409–18. [PubMed: 22508388]

31. Pirinen M, Donnelly P, Spencer CC. Including known covariates can reduce power to detect genetic effects in case-control studies. *Nat Genet.* 2012; 44:848–51. [PubMed: 22820511]
32. Zaitlen N, et al. Informed conditioning on clinical covariates increases power in case-control association studies. *PLoS Genet.* 2012; 8:e1003032. [PubMed: 23144628]
33. Falconer DS. The inheritance of liability to diseases with variable age of onset, with particular reference to diabetes mellitus. *Ann Hum Genet.* 1967; 31:1–20. [PubMed: 6056557]
34. Lee SH, Wray NR, Goddard ME, Visscher PM. Estimating missing heritability for disease from genome-wide association studies. *Am J Hum Genet.* 2011; 88:294–305. [PubMed: 21376301]
35. Jostins L, et al. Host-microbe interactions have shaped the genetic architecture of inflammatory bowel disease. *Nature.* 2012; 491:119–24. [PubMed: 23128233]
36. Lee SH, et al. Estimation and partitioning of polygenic variation captured by common SNPs for Alzheimer's disease, multiple sclerosis and endometriosis. *Hum Mol Genet.* 2013; 22:832–41. [PubMed: 23193196]
37. Devlin B, Roeder K. Genomic control for association studies. *Biometrics.* 1999; 55:997–1004. [PubMed: 11315092]
38. Lango Allen H, et al. Hundreds of variants clustered in genomic loci and biological pathways affect human height. *Nature.* 2010; 467:832–8. [PubMed: 20881960]
39. Meuwissen TH, Hayes BJ, Goddard ME. Prediction of total genetic value using genome-wide dense marker maps. *Genetics.* 2001; 157:1819–29. [PubMed: 11290733]
40. Erbe M, et al. Improving accuracy of genomic predictions within and between dairy cattle breeds with imputed high-density single nucleotide polymorphism panels. *J Dairy Sci.* 2012; 95:4114–29. [PubMed: 22720968]
41. Zhou X, Carbonetto P, Stephens M. Polygenic modeling with bayesian sparse linear mixed models. *PLoS Genet.* 2013; 9:e1003264. [PubMed: 23408905]
42. Yang J, Lee SH, Goddard ME, Visscher PM. GCTA: a tool for genome-wide complex trait analysis. *Am J Hum Genet.* 2011; 88:76–82. [PubMed: 21167468]



### 1. MLMe increases power but MLMi reduces power vs. linear regression

We report  $\chi^2$  association statistics at 500 causal markers for MLMi vs. linear regression and MLMe vs. linear regression for one simulation with genotypes from ref.<sup>24</sup> data and simulated phenotypes for  $N=10,000$  samples. For MLMe, the 500 causal markers were always excluded from computing the GRM.



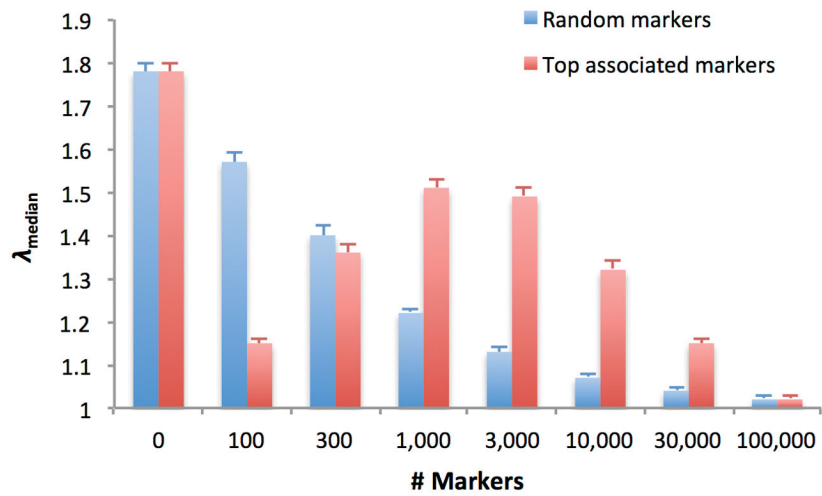


**Figure 2. Effectiveness of MLM using  $M_R$  random or  $M_T$  top associated markers in correcting for stratification**

We report the average  $\lambda_{\text{median}}$  ( $\pm$  standard error) in 100 simulations with population stratification based on  $N=10,000$  samples,  $M=100,000$  markers, two discrete subpopulations with  $F_{ST}=0.005$ , and a mean trait difference of 0.25 standard deviations between subpopulations. Calibration of small P-values is reported in Supplementary Table 4.

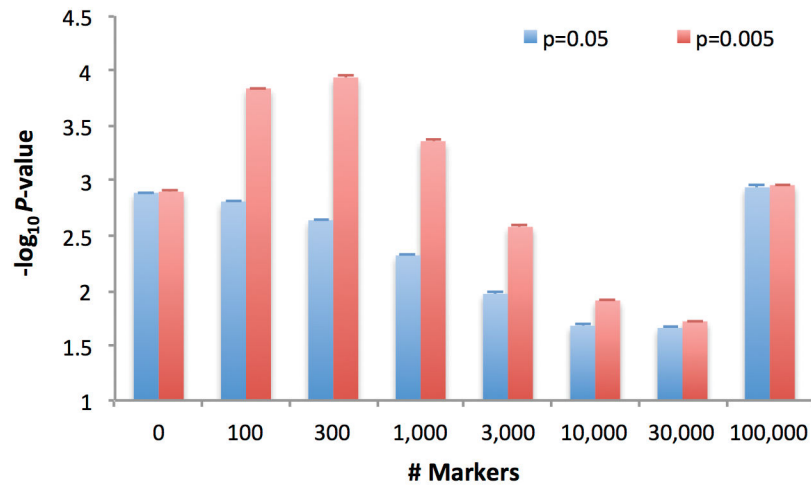


**Figure 3. Effectiveness of MLM using  $M_T$  top associated markers in increasing study power**  
 We report average  $-\log_{10} P$ -values ( $\pm$  standard error) at causal markers in 100 simulations based on  $N=10,000$  samples,  $M=100,000$  markers, and fraction  $p=0.05$  or  $p=0.005$  of causal markers. Power to detect significant associations at different P-value thresholds is reported in Supplementary Table 5.

**Table 1**  
**Computational cost of EMMAX, FaST-LMM, GEMMA, GRAMMAR-Gamma and GCTA**

For each method we list the computational cost of each step (see main text).

	<b>Building GRM</b>	<b>Variance components</b>	<b>Association statistics</b>
EMMAX	$O(MN^2)$	$O(N^3)$	$O(MN^2)$
FaST-LMM*	$O(MN^2)$	$O(N^3)$	$O(MN^2)$
GEMMA	$O(MN^2)$	$O(N^3)$	$O(MN^2)$
GRAMMAR-Gamma	$O(MN^2)$	$O(N^3)$	$O(MN)$
GCTA	$O(MN^2)$	$O(N^3)$	$O(MN^2)$

\* If  $M < N$ , the computational cost of FaST-LMM can be reduced to  $O(M^2N)$ .

**Table 2**  
**MLMe increases power but MLMi decreases power vs. linear regression**

In scenario I, we report average  $\chi^2$  association statistics ( $\pm$  standard errors) at 500 candidate causal markers for linear regression, MLMi and MLMe, averaged across 100 simulations based on simulated genotypes. In scenario II, we report average  $\chi^2$  association statistics ( $\pm$  standard errors) at 200 causal markers for simulations based on ref. <sup>24</sup> genotype data with simulated phenotypes. In both scenarios, expected values based on theoretical derivations are given in parentheses. More details including simulations at other values of  $N$  and  $M$ , results for all markers, power to detect significant associations at different  $P$ -value thresholds, and the equations to calculate the expected values are provided in Supplementary Table 3.

# samples ( $N$ )	#markers ( $M$ )	Linear regression (Expected value)	MLMi (Expected value)	MLMe <sup>&amp;</sup> (Expected value)
Scenario I: Simulated unlinked markers				
10,000	10,000	10.93 $\pm$ 0.03 (11.00)	9.81 $\pm$ 0.01 (10.05 <sup>*</sup> )	13.27 $\pm$ 0.03 (13.36)
10,000	100,000	11.20 $\pm$ 0.03 (11.00)	10.97 $\pm$ 0.02 (10.09 <sup>*</sup> )	11.40 $\pm$ 0.03 (11.25)
Scenario II: Simulations based on real genotype data <sup>24</sup>				
10,000	133,036	26.99 $\pm$ 0.10 (26.00)	21.44 $\pm$ 0.05 (19.85)	28.42 $\pm$ 0.10 (29.08)

<sup>\*</sup> For MLMi, the  $h_g^2$  of markers included in the GRM is 100%, and the derivation is much less accurate. However, the derivation is much more accurate at lower values of  $h_g^2$  (Supplementary Table 3a).

<sup>&</sup> The 500 candidate causal markers were always excluded from calculating the GRM in scenario I and the MLMe analysis was performed using GCTA-LOCO in scenario II.

**Table 3**  
**MLMe decreases power vs. linear regression under case-control ascertainment**

We report average  $-\log_{10}P$ -values ( $\pm$  standard error) at causal markers for linear regression and MLMe, averaged across 100 simulations with  $p=0.05$  and each candidate marker explaining  $10/N$  of observed-scale variance. Results for different values of  $N$ ,  $M$ ,  $p$  and the proportion of variance explained by each candidate marker are reported in Supplementary Table 8, which also reports the power to detect significant associations at different P-value thresholds.

# samples ( $N$ )	#markers ( $M$ )	Disease prevalence ( $f$ )	Linear regression	MLMe
10,000	10,000	0.001	$3.06 \pm 0.15$	$2.22 \pm 0.12$
10,000	10,000	0.01	$3.04 \pm 0.16$	$2.64 \pm 0.14$
10,000	10,000	0.1	$3.04 \pm 0.17$	$3.06 \pm 0.17$
10,000	100,000	0.001	$2.96 \pm 0.16$	$2.78 \pm 0.16$
10,000	100,000	0.01	$2.66 \pm 0.14$	$2.54 \pm 0.13$
10,000	100,000	0.1	$3.24 \pm 0.16$	$3.26 \pm 0.16$

Table 4

**Empirical results in MS and UC datasets**

We report average  $\chi^2$  association statistics for all markers ( $\lambda_{\text{median}}$  in parentheses) and for published associated markers, for each method (see main text). The FaST-Top method selected  $M_T=2,000$  top markers for MS and  $M_T=400$  top markers for UC, and the FaST-TopX method selected  $M_T=2,800$  top markers for MS and  $M_T=3$  top markers for UC.

	LR	PCA	MLMi	MLMe&	FaST-4K	FaST-Top	FaST-TopX
MS, 360,557 SNPs ( $\lambda_{\text{median}}$ )	3.95 (3.86)	1.25 (1.23)	0.99 (0.97)	1.23 (1.20)	1.86 (1.80)	1.42 (1.39)	1.41 (1.39)
MS, 75 published SNPs	18.50	10.20	8.90	11.30	13.98	10.99	10.56
UC, 458,560 SNPs ( $\lambda_{\text{median}}$ )	1.16 (1.16)	1.11 (1.10)	1.00 (0.99)	1.10 (1.09)	1.14 (1.13)	1.08 (1.09)	1.16 (1.15)
UC, 24 published SNPs	14.06	13.63	12.11	13.43	13.99	10.75	14.09

& The MLMe analysis was performed using GCTA-LOCO.